3818 *Macromolecules* **2009**, *42*, 3818−3822

Dynamics of PMMA−PHSA Hard Spheres under External Electric Field at Low Temperatures: a Singular Dynamic Light Scattering Experiment

Fernando C. Giacomelli,[§,†,‡] Nádya P. da Silveira,[†] and Petr Štěpánek*[,‡]

*Institute of Chemistry, Universidade Federal do Rio Grande do Sul, Av. Bento Gonçalves 9500,
91501-970 Porto Alegre, Brazil, and Institute of Macromolecular Chemistry, Heyrovský Sq. 2,
162 06 Prague 6, Czech Republic*

Received February 24, 2009; Revised Manuscript Received March 31, 2009

ABSTRACT: The effect of the temperature on the dynamic behavior of PMMA−PHSA hard spheres under the influence of external electric field is described. By using a very uncommon light scattering setup for low temperature measurements, it was possible to study the influence of the temperature in the diffusion of particles under external electric field in a wide range (from 223 to 323 K). Previously, it was verified that the electric field induces an increment in the relaxation rate—Γ—(measured by dynamic light scattering) related to the movement of PMMA−PHSA hard spheres suspended in different solvents (*Macromol. Symp.* 2006, *245−246*, 457.). In that case, a qualitative E^2 dependence of Γ was observed and it was more pronounced in solvents having higher dielectric constant. Herein, it was evidenced that the effects of the electric field are clearer when the same measurements are done in temperatures as low as possible. The reduction in the temperature of the system decreases the thermal energy linked to the Brownian motion of the particles and the electric field influence is enhanced. The enhancement in the current case is also linked to the increase in the dielectric constant of the solvent THF, used to suspend the hard spheres, as the temperature reduces.

Introduction

Throughout the literature, one can find topical contributions focused on different measurements with *in situ* applied electric field. Microscopic and small-angle X-ray scattering (SAXS) experiments were recently explored. Putaux et al.[1] use light microscopy to demonstrate the alignment of cellulose fibers suspended in toluene when an external electric field was applied through the system and Li et al.[2] verified, by using transmission and scanning electron microscopy, that applying an AC electric field, highly long-range ordered aggregates are generated from PS−PAA micelles in aqueous solution. SAXS measurements were recently used to illustrate the alignment of domains in highly concentrated block copolymers solutions,[3] where the influence of initial order[4] and dielectric contrast between blocks[5] were deeply discussed. On a similar way, Russell et al. have been studying through SAXS the electric field orientation of bulk block copolymers[6,7] and the electric field alignment of symmetric[8] and asymmetric[9] block copolymer thin films. They also observed a sphere-to-cylinder transition in PS-*b*-PMMA thin films,[10] as suggested theoretically.[11,12] We shall show, in a forthcoming paper, evidences of a cubic-to-hexagonal transition in a solution of diblock copolymer dissolved in partially miscible solvents through the application of electric field as well.[13] Such pronounced effects of electric field on the structure of polymeric materials in comparison with the effects on small solvent molecules are mainly due to the higher molecular weight of the polymers and to the associated low entropy.

On the other hand, a very limited number of contributions can be found focusing on *in situ* applied electric field during dynamic light scattering measurements,[14−17] and some of them[15,16] seem to bring different suggestion for the behaviors observed. The scarce number of contributions in this field might be, among other issues, related to the difficulties to prepare a reliable experimental setup to hinder light reflections and the need to avoid electrophoretic effects, which is possible only when the studied systems have some special characteristics.[18] It is worth mentioning that the PMMA−PHSA hard spheres used in the current experiments were uncharged and therefore they do not move linearly under an applied electric field as is the case in electrophoretic light scattering (ELS) experiments. In ELS, charged colloidal particles are placed under electric field and their linear velocity can be determined by optically measuring the Doppler shift of the frequency of the incident beam. The frequency shift can be further correlated to the electrophoretic mobility and zeta potential of the particles. Our idea in the experiments described below was to understand how the Brownian motion of uncharged particles is affected by electric field.

Some theoretical contributions can also be found;[19−21] however, the electric field range we can access experimentally falls well below that one demonstrated theoretically.

Presently, we have focused on the study of the dynamic behavior and structural changes in different polymeric systems under the application of external forces. Efforts have been made in order to completely understand and check experimentally the influence of external electric fields in the diffusion behavior of particles approaching nanoscale. Recently, it was studied the behavior of solutions containing a new synthesized triblock copolymer dissolved in different solvents, where it was possible to observe the influence of size and dielectric contrast in the dynamics of different particles in solution.[22] It was also demonstrated that it is possible to achieve a huge increase in the diffusion rate of rather large particles ($R_H \sim 140$ nm) under external electric field, only varying the dielectric constant of the liquid matrix where they are suspended.[23] This work was performed using PMMA−PHSA hard spheres as a model system.

Following our previous results, we show currently the influence of the temperature in the dynamic behavior of the same

---

* Corresponding author. E-mail: stepan@imc.cas.cz. Telephone: +420 2 96809211. Fax: +420 2 96809410.

[†] Institute of Chemistry, Universidade Federal do Rio Grande do Sul.

[‡] Institute of Macromolecular Chemistry.

[§] Current address: LNLS, Laboratório Nacional de Luz Síncrotron, Giuseppe Máximo Scolfaro 10000, 13083-970, Campinas-SP, Brazil.

10.1021/ma900423y CCC: $40.75

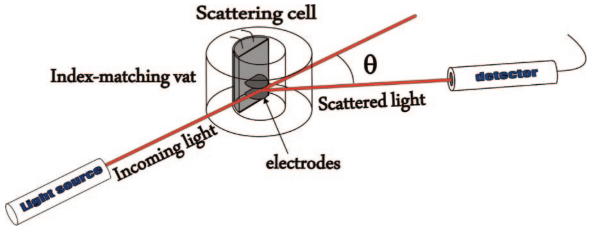

Figure 1. View of the configuration for DLS measurements with *in situ* applied electric field.

PMMA−PHSA hard spheres suspended in THF and under external electric field, using the resources of dynamic light scattering measurements (DLS). As detailed in the experimental section, it was possible to reach temperatures as low as 223 K (−50 °C). We shall show that reducing the temperature of the system, the effect of the electric field in the dynamic behavior of the hard spheres is enhanced due to two superimposing factors: the reduction on the thermal energy of the system and the increase in the dielectric constant of the solvent THF.

Experimental Procedures

The System. The particles comprise a core made of amorphous poly(methyl methacrylate) (PMMA) stabilized by a grafted thin layer (~5 nm) of poly(12-hydroxystearic acid) (PHSA). The latter avoids aggregation due to van der Waals forces. The detailed particles preparation is provided elsewhere.[24] They were extensively used as a colloidal model system of hard spheres by Pusey et al.,[25−27] and they show a very interesting phase behavior depending on their volume fraction is *cis*-decalin. Only below the volume fraction of $\phi = 0.494$ they behave as a completely disordered fluid.[26]

Sample Preparation. From a stock suspension of PMMA−PHSA hard spheres in *cis*-decalin ($\phi = 0.33$), a 200 μL aliquot was dropwise added into 5 mL of the organic solvent tetrahydrofuran (THF). The solvent was of analytical grade purchased from Aldrich. Thus, the resulting volume fraction of PMMA−PHSA hard spheres in the solvent was equal to $\phi = 0.013$. Since the only technique used was standard DLS, this was the maximum amount of hard spheres we could have in suspension in order to avoid multiple scattering. The sample in such a case was still completely transparent.

During the course of the experiments, the particles remained very stable and no processes of aggregation were identified neither the swelling of the PMMA−PHSA hard spheres was evidenced by DLS. The time measurement to cover the range of temperatures accessed was roughly 2 h, and the size of the particles remained within an experimental error during that period ($R_H = 220 \pm 10$ nm) as detailed hereafter in the Results and Discussion.

Electric Field Apparatus. A dc external electric field was applied through the suspension using a home-built capacitor schematically represented in Figure 1.

As shown, the electric field is pointed perpendicular to the beam. The capacitor was constructed using polyacetal remnant as support for two parallel circular copper plates (electrodes) with a black finish to avoid undesirable light reflections. The electrodes separation was chosen as 4.0 mm. External dc electric fields up to 200 kV m^{-1} were applied using a Matsusada high voltage power supply. During the experiments, the temperature, applied voltage and the current density were carefully monitored.

Low Temperature Setup. A home-built apparatus was used to reach the very low temperatures. To do so, a heater is placed inside a bottle of liquid nitrogen producing vapors that flow through the entire double wall scattering vat, as depicted in Figure 2.

The inner copper block in the sample holder is electrically heated by a temperature controller Lakeshore model 330. The flow of nitrogen vapors is tuned so that by simultaneous action of cooling and heating any temperature in the range 200 to 298 K can be adjusted. The index matching solvent was a mixture of toluene and 2-propanol (80/20 v/v). A small amount of 2-propanol was used in order to avoid the presence of water crystals in the toluene phase at very low temperatures. The temperature in the vat with the index matching liquid is homogeneous within 0.2 K and is stable in time within 0.1 K down to 193 K.

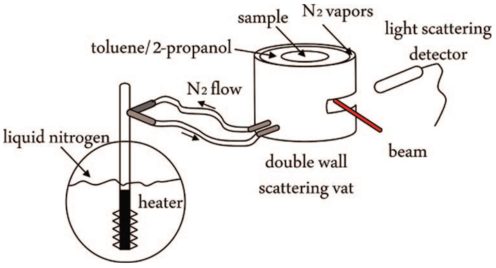

Figure 2. Configuration for DLS measurements at low temperatures.

Dynamic Light Scattering Measurements and Data Analysis. The home-built DLS instrument is equipped with a Uniphase 22 mW He−Ne laser ($\lambda = 632.8$ nm) as light source and an ALV 5000/E correlator with single-mode fiber optics. The measurements were carried out at $\theta = 90°$.

The measured intensity autocorrelation functions $g_2(t)$ were analyzed using the algorithm REPES (incorporated in the GENDIST program) which employs the inverse Laplace transformation according to eq 1.[28]

$$g_2(t) - 1 = Z\Big[\int A(\tau)\exp(-t/\tau)\,\mathrm{d}\tau\Big]^2 \qquad (1)$$

where t is the delay time of the correlation function, τ the decay time and Z is an instrumental parameter. The resulting $A(\tau)$ is a distribution of relaxation times that consists generally of several peaks representing individual dynamic processes. Herein, the distributions of the relaxation times are shown in the equal area representation[29] as $\tau A(\tau)$ vs $\log \tau$.

The mean relaxation time τ or the relaxation frequency Γ ($=\tau^{-1}$) characteristic of a dynamic process can be quantitatively associated to an apparent diffusion coefficient (D) according to eq 2.

$$D = \frac{\Gamma}{q^2} \qquad (2)$$

Finally, the hydrodynamic radius (R_H) is derived from the determined value of D using the well-known Stokes−Einstein relation:

$$R_H = \frac{k_B T}{6\pi\eta D} \qquad (3)$$

k_B is the Boltzmann constant, T is the absolute temperature, and η is the viscosity of the solvent.

Results and Discussion

Figure 3 shows the distribution of relaxation times for PMMA−PHSA hard spheres suspended in THF at the lower (223 K) and upper (323 K) limit temperatures accessed, and in absence of electric field.

As can be seen, the dynamic light scattering measurements followed by the REPES analysis were able to detect only a single and narrow distribution at both temperatures. In other words, only the dynamic process related to the diffusion of the PMMA−PHSA hard spheres in the organic solvent can be seen in the full range of temperature.

The THF viscosity was calculated using eq 4. This equation was constructed by fitting tabulated values.[30]

$$\log \eta_{THF} = -4.82 + \frac{4761}{(T + 1034)} \qquad (4)$$

The temperature is given in °C and the viscosity in mPa.s. The values of Γ_0, related to the diffusion constant of the PMMA−PHSA hard spheres at zero electric field, are linearly dependent on T/η_{THF} (Figure 4, top) and the determined R_H of the scattering objects remain constant ~ 220 nm over the range of temperature accessed (Figure 4, bottom).

This is an extremely important finding, since as we shall show hereafter, the volume of the particles is crucial to understand the effects of electric field in their dynamic behavior, and it should remain constant in order to evaluate the other parameters of interest.

Figure 5 shows the E^2 dependence of Γ_E/Γ_0 for different temperatures (Γ_E is the relaxation frequency monitored by DLS under electric field having different intensities). For the sake of better visualization, we show the profile of only three checked temperatures. One can notice that the reduction in the temperature of the system enhances the E^2 dependence of Γ_E/Γ_0.

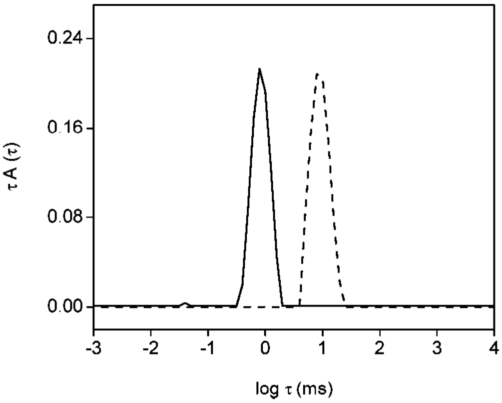

Figure 3. Distributions of relaxation times for PMMA−PHSA hard spheres suspended in THF at 223 K (dotted line) and 323 K (solid line) and $E = 0$ kV m^{-1}.

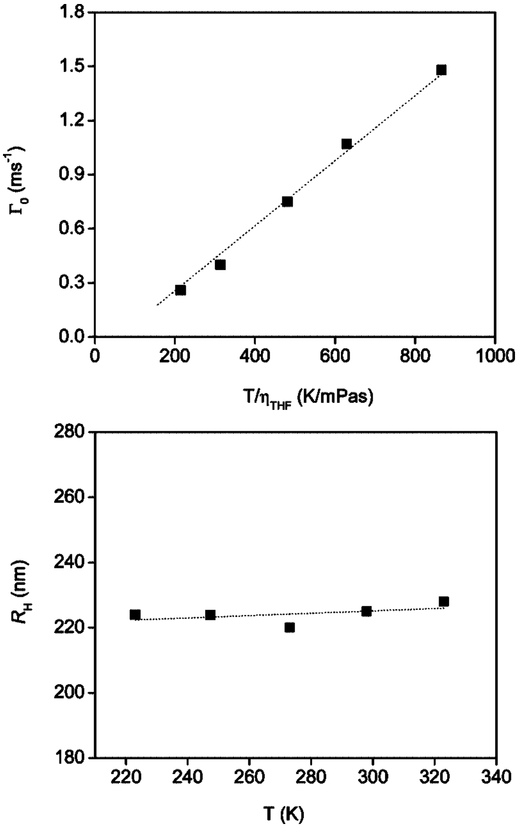

Figure 4. Γ_0 vs T/η_{THF} for PMMA−PHSA hard spheres suspended in THF (top) and R_H determined using the Stokes−Einstein equation at different temperatures (bottom).

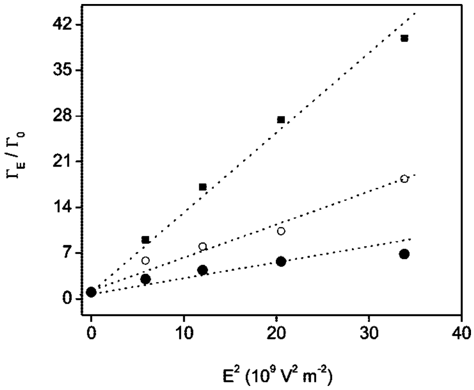

Figure 5. E^2 dependence of Γ_E/Γ_0 for PMMA−PHSA hard spheres suspended in THF at 223 K (filled squares); 273 K (open circles) and 323 K (filled circles).

Since our first contribution in this field, we have attempted to understand the mechanisms leading to such increase in the relaxation frequency monitored by DLS and related to the diffusion of the particles under electric field by taking into account the competition between the two energies present: the thermal energy responsible for the Brownian motion of the particles that it is governed by the kinetic-molecular theory of heat (existing also at zero electric field) and the electric energy imposed by the external electric field: when an electric field crosses the suspension containing the scattering objects, it generates a dipole moment (p) in the particles. The dipole moment produces an additional electric energy that contributes to the movement of them ($E_{electric} = p.E$). The induced dipole moment (p) can be quantitatively described as:

$$p = 4\pi\varepsilon\varepsilon_0\beta R^3 E \tag{5}$$

wherein ϵ_0 is the permittivity of the free space (8.854×10^{-12} F m^{-1}) and β is a dielectric mismatch parameter that involves the dielectric constant of the hard spheres (it is used the dielectric constant of the main particle component PMMA − $\epsilon_{\mathrm{PMMA}} = 3.6$)[31] and the dielectric constant of the solvent THF − $\epsilon_{\mathrm{THF}} = 7.52$.[32]

$$\beta = \frac{\varepsilon_{\mathrm{PMMA}} - \varepsilon_{\mathrm{THF}}}{\varepsilon_{\mathrm{PMMA}} + 2\varepsilon_{\mathrm{THF}}} \tag{6}$$

The competition between the thermal and the electric energy induced by the dipole moment can be estimated by eq 7.

$$\frac{E_{\mathrm{electric}}}{E_{\mathrm{thermal}}} = \frac{pE}{k_B T} = \frac{4\pi\varepsilon\varepsilon_0\beta R^3 E^2}{k_B T} \tag{7}$$

The linear behavior seen in Figure 5 and the fact that the effects of electric field are visible only in the dynamic behavior of particles with a relatively large size[22,23] (due to the fact that according to eq 7, $E_{\mathrm{electric}} \sim R^3$) are consistent with the idea of the generation of a dipole moment in the particles being responsible for the effects observed. Given that in the current case $\beta < 0$ (that is to say $\epsilon_{\mathrm{THF}} > \epsilon_{\mathrm{PMMA}}$), the dipole moment acquired by them has an opposite direction relative to the direction of the applied electric field. In such a case, the PMMA−PHSA hard spheres should experience a torque to overcome the unstable situation as well as to align their dipole moment with the electric field.[33] However, as a consequence of this motion, the dipole moment and the electric field become normal. In such configuration, i.e., when the dipoles are side-by-side, they repel each other, and consequently, it generates a repulsion between particles in close proximity, as demonstrated by the cartoon of Figure 6.

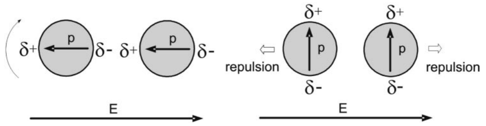

Figure 6. Cartoon describing the behavior of PMMA−PHSA hard spheres under electric field ($\beta < 0$).

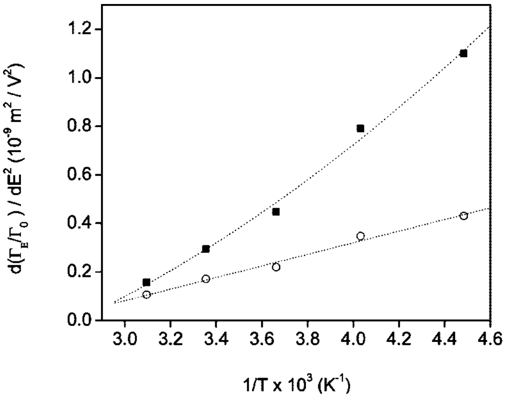

Figure 7. $1/T$ dependence of $d(\Gamma_E/\Gamma_0)/dE^2$ (filled squares) and the same values divided by $|\epsilon_{THF}\beta|$ (open circles) for PMMA−PHSA hard spheres suspended in THF.

This qualitative discussion can explain the absence of chaining of the hard spheres such as in an electrorheological fluid. Indeed, it might occur when $\beta > 0$, which means, for the same particles suspended in a solvent with dielectric constant smaller than ϵ_{PMMA}, where the dipole moment acquired by them and the electric field will have the same directions. Thus, we claim that the values of Γ_E monitored are related to superimposing contributions coming from the classical Brownian motion of the particles and the repulsion between them.

Even though the viscosity has a huge influence in the Γ_0 values at distinct temperatures, when the values under external electric field are normalized by Γ_0, the increase in Γ_E/Γ_0 vs. E^2 at different temperatures can be compared and as already mentioned, it can be noticed that the effects of the electric field acting on the movement of the particles are more pronounced as the temperature is reduced.

According to eq 7, one reason for such effect is linked to the reduction in the thermal energy of the system. From 323 K and going down to 223 K, a reduction in the thermal energy in the order of 40% is achieved and it might be expected that for an equal electric field intensity applied through the suspension, the effects of such external force should be more pronounced.

Figure 7 shows the variation in the slope $d(\Gamma_E/\Gamma_0)/dE^2$ against the reciprocal of the temperature (filled squares) and the same values divided by $|\beta\epsilon_{THF}|$ as discussed later on (open circles).

Clearly, it can be seen an upward profile of the black square points. Taking into account eq 7, it should be expected a linear profile if the enhancement on the electric field effects was entirely related to the reduction in the thermal energy of the system. Our experimental result means that not only the reduction in the thermal energy but also some other parameter(s) has a visible effect on the dynamics of the particles. It was showed in Figure 4 (bottom) that the particles preserve the same size, even when the temperature of the system was reduced down to 223 K. The possibility of swelling was checked at 323 K for 3 h and a negligible increase in size was noticed ($R_H \sim$ 218−222 nm) which is within the experimental error. Therefore, the values of dielectric constant of the components (ϵ_{THF} and ϵ_{PMMA}) must be checked against the temperature.

The variation on the dielectric constant with the temperature is different for polar and nonpolar polymers. Generally, for strong polar polymers, the dielectric constant increases with the temperature, whereas it is independent of the temperature for nonpolar polymers.[36] PMMA has a weak polar nature; however, its dielectric constant is mainly independent of the temperature. Unfortunately, we could not find values of dielectric constant for PMMA in the range of low temperatures we were working on. Nevertheless, from 303 to 383K, the dielectric constant increases by less than 2%, about 0.06 (from 3.18 to 3.24) for values determined at 10 kHz as given in Figure 8 (top). The enhancement in polarization is responsible for this little increase in dielectric constant of PMMA over the temperature.[34] The polymer PMMA has a glass transition temperature at about 100 °C.[31] Regarding that no phase transitions is expected in the range of temperature studied and also that only a negligible difference is reported in ϵ_{PMMA} in a wide interval of temperature (even close to its glass transition), it can be assumed that the effects observed on the dynamics of the hard spheres under external electric field is not related to changes in ϵ_{PMMA}.

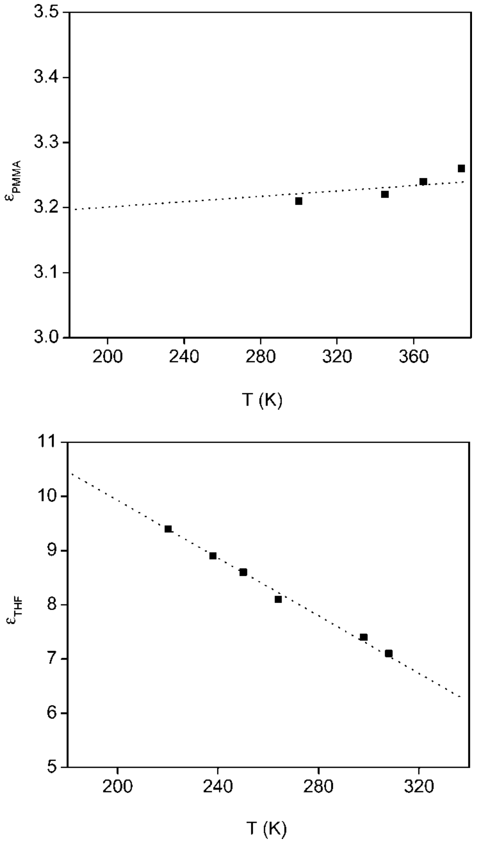

Figure 8. Temperature dependence of ϵ_{PMMA} (top)[34] and ϵ_{THF} (bottom).[35]

On the other hand, the solvent THF shows a considerable change in dielectric constant over the temperature. Figure 8 (bottom) shows values very close to the range of temperature studied. From 220 to 308 K, a reduction in the dielectric constant is noticed for THF (from 9.4 to 7.1). Taking into account the values of ϵ_{PMMA} and ϵ_{THF}, it was determined the values of $\epsilon_{THF}\beta$ against $1/T$. As depicted in Figure 9, its modulus increases linearly as $1/T$ increases.

Thus, the upward profile showed in Figure 7 (filled squares) is related to two superimposing effects that enhance the Γ_E values of the PMMA−PHSA hard spheres determined from DLS: the reduction in the temperature, which by consequence enhances the relative contribution of $E_{electric}$ in the dynamics of the scattering objects and at the same time, an increase in the values of ϵ_{THF}, resulting in a even more pronounced contribution of $E_{electric}$ as the temperature is reduced, due to the increase in

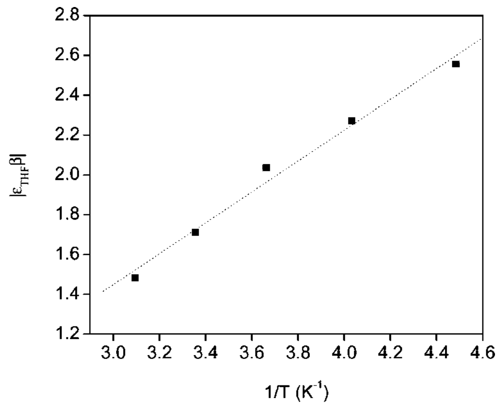

Figure 9. $1/T$ dependence of $|\epsilon_{THF}\beta|$ for PMMA−PHSA hard spheres suspended in THF.

the parameter $|\epsilon_{THF}\beta|$. We propose the qualitative relation given in eq 8 to describe such a case.

$$\frac{d(\Gamma_E/\Gamma_0)}{dE^2} \sim |\varepsilon_{THF}\beta| \frac{1}{T} R^3 \qquad (8)$$

The division of the values of $d(\Gamma_E/\Gamma_0)/dE^2$ by the modulus of $\epsilon_{THF}\beta$ led to a straight line and the upward curvature disappears (Figure 7, open circles). Such simple procedure is efficient in order to disconnect the contribution of the increase in ϵ_{THF} and of the reduction in the temperature in the Γ_E monitored. Finally, one can also notice that as the temperature is reduced (increase in $1/T$), the effect of the increase in ϵ_{THF} somehow overcome the effect of the reduction in the temperature itself. In other words, the increase in $d(\Gamma_E/\Gamma_0)/dE^2$ is more related to the increase in $|\epsilon_{THF}\beta|$. On the other way round, when the temperature increases (reduction in $1/T$), both effects are reduced and they become comparable in the contribution for the final value of $d(\Gamma_E/\Gamma_0)/dE^2$. It also means that there should be a higher temperature (probably higher than the boiling point of THF = 78 °C) where the electric field effect would vanish.

Conclusions

Herein, we have experimentally observed the effect of the temperature in the dynamic behavior of PMMA−PHSA hard spheres suspended in THF and under an external electric field. The electric field range comprehended values between 0 (unapplied) and 200 kV m^{-1} and the temperature dependence was studied in a wide range (from 223 to 323 K). The work was done by using a home-built capacitor for *in situ* applied electric field during DLS measurements and using a very uncommon home-built light scattering instrument where it was possible to reach very low temperatures.

It was noticed that the effects of the electric field are clearer and more pronounced observed when the temperature of the system was reduced, which means a reduction in its thermal energy. The reduction in the temperature led in the current case to a huge increase in Γ_E. It was demonstrated that the enhancement in Γ_E is related to two superimposing contributions: an enhancement in the ratio between the electric and the thermal energy promoted by the reduction of the temperature and an enhancement on the dielectric constant of the solvent (and as consequence in $|\epsilon_{THF}\beta|$) as the temperature is reduced. Both effects could be at least qualitatively separated. The values of Γ_E come from a contribution of the Brownian motion of the particles and from the repulsion between them.

Acknowledgment. We acknowledge support by the Grant Agency of the Academy of Sciences of the Czech Republic (Grant No. 202/09/2078). F.C.G. thanks CNPq-Brazil for the fellowship granted. Abdellatif Moussaïd is acknowledged for the given sample.

References and Notes

(1) Bordel, D.; Putaux, J. L.; Heux, L. *Langmuir* **2006**, *22*, 4899–4901.
(2) Li, G.; Shi, L.; Ye, Q.; Zhou, W.; Tian, J. *Colloid Polym. Sci.* **2006**, *284*, 1179–1183.
(3) Böker, A.; Knoll, A.; Elbs, H.; Abetz, V.; Muller, A. H. E.; Krausch, G. *Macromolecules* **2003**, *35*, 1319–1325.
(4) Schmidt, K.; Boker, A.; Zettl, H.; Schubert, F.; Hansel, H.; Fischer, F.; Weiss, T. M.; Abetz, V.; Zvelindovsky, A. V.; Sevink, G. J. A.; Krausch, G. *Langmuir* **2005**, *21*, 11974.
(5) Böker, A.; Schmidt, K.; Knoll, A.; Zettl, H.; Hansel, H.; Urban, V.; Abetz, V.; Krausch, G. *Polymer* **2006**, *47*, 849–857.
(6) Thurn-Albrecht, T.; DeRouchey, J.; Russell, T. P.; Kolb, R. *Macromolecules* **2002**, *35*, 8106.
(7) DeRouchey, J.; Thurn-Albrecht, T.; Russell, T. P.; Kolb, R. *Macromolecules* **2004**, *37*, 2538.
(8) Xu, T.; Zhu, Y.; Gido, S. P.; Russell, T. P. *Macromolecules* **2004**, *37*, 2625.
(9) Xu, T.; Zvelindovsky, A. V.; Sevink, G. J. A.; Lyakhova, K. S.; Jinnai, H.; Russell, T. P. *Macromolecules* **2005**, *38*, 10788.
(10) Xu, T.; Zvelindovsky, A. V.; Sevink, G. J. A.; Gang, O.; Ocko, B.; Zhu, Y.; Gido, S. P.; Russell, T. P. *Macromolecules* **2004**, *37*, 6980.
(11) Matsen, M. W. *J. Chem. Phys.* **2006**, *124*, 074906.
(12) Tsori, Y.; Tournilhac, F.; Andelman, D.; Leibler, L. *Phys. Rev. Let.* **2003**, *90*, 145504/1.zprint>.
(13) Stepánek, P.; Giacomelli, F. C.; da Silveira, N. P. Tuzar, Z.; Kadlec, P. manuscript in preparation.
(14) Price, C.; Deng, N.; Lloyd, F. R.; Li, H.; Booth, C. *J. Chem. Soc., Faraday Trans.* **1995**, *91*, 1357.
(15) Sun, Z.; Wang, C. H. *Macromolecules* **1999**, *32*, 2605.
(16) Wang, C. H.; Huang, Q. R. *J. Chem. Phys.* **1997**, *106*, 2819.
(17) Fujii, S.; Isojima, T.; Sasaky, N.; Hamano, K. *Colloid Polym. Sci.* **2001**, *279*, 252.
(18) Berne, B. J.; Pecora, R. *Dynamic Light Scattering*; John Wiley & Sons: New York, 1976.
(19) Lipson, J. E. G.; Stockmayer, W. H. *J. Chem. Phys.* **1988**, *89*, 3373.
(20) Lipson, J. E. G.; Stockmayer, W. H. *J. Chem. Phys.* **1989**, *90*, 1950.
(21) Chen, C.; Hua, C.; Wu, C. *Macromol. Theory Simul.* **2001**, *10*, 644.
(22) Giacomelli, F. C.; Riegel, I. C.; Petzhold, C. L.; da Silveira, N. P. *Macromolecules* **2008**, *41*, 2677.
(23) Giacomelli, F. C.; Pereira, F. V.; da Silveira, N. P.; Moussaid, A. *Macromol. Symp.* **2006**, *245−246*, 457.
(24) Antl, L.; Goodwin, J. W.; Hill, R. D.; Ottewill, R. H.; Owens, S. M.; Papworth, S.; Waters, J. A. *Colloids Surf.* **1986**, *17*, 67.
(25) Petekidis, G.; Moussaid, A.; Pusey, P. N. *Phys. Rev. E* **2002**, *66*, 051402.
(26) Petekidis, G.; Pusey, P. N.; Moussaid, A.; Egelhaaf, S.; Poon, W. C. K. *Physica A* **2002**, *306*, 334.
(27) Pham, K. N.; Puertas, A. M.; Bergenholtz, J.; Egelhaff, S.; Moussaid, A.; Pusey, P. N.; Schofield, A. B.; Cates, M. E.; Fuchs, M.; Poon, W. C. K. *Science* **2002**, *296*, 104.
(28) Jakes, J. *Collect. Czech. Chem. Commun.* **1995**, *60*, 1781.
(29) Stepánek, P. In *Dynamic light scattering: The Method and Some Applications*; Brown, W., Ed.; Oxford Science Publications: Oxford, U.K., 1993.
(30) *Angew. Z. Phys.* **1955**, *372*, 376.
(31) Brandrup, J.; Immergut, E. H. *Polymer Handbook*; 3rd ed.; Wiley: New York, 1991.
(32) David, R. L. *Handbook of Chemistry and Physics*, 78th ed.; CRC Press: New York, 1997−1998.
(33) Boissy, C.; Allen, P.; Foulc, J. N. *J. Electrost.* **1995**, *35*, 13.
(34) Mittal, A.; Jain, V.; Mittal, J. *Asian J. Chem.* **2001**, *3*, 1216.
(35) Gee, N.; Shinsaka, K.; Dodelet, J. P.; Freeman, G. R. J. *Chem. Termodyn.* **1986**, *18*, 221.
(36) Shekar, B. C.; Na, M.; Lee, J.; Rhee, S. *Mol. Cryst. Liq. Cryst.* **2004**, *424*, 43.

MA900423Y